THE INITIATION AND PROPAGATION OF SMALL DEFECTS IN FRETTING FATIGUE

K. J. NIX AND T. C. LINDLEY*

The fretting fatigue properties of 3½NiCrMoV steel specimens in contact with 1CrMo steel fretting pads have been investigated. The conditions for the initiation of small defects have been determined by carrying out interrupted tests. Small defects less than 0.2 mm in depth can be present at stresses well below the fretting fatigue limit. Their size is governed by the frictional forces between the contacting materials and is essentially independent of applied fatigue stresses. The nature of the small defects has been investigated metallographically and fractographically. Their significance in relation to fretting fatigue assessment is discussed.

INTRODUCTION

Fretting fatigue is the reduction in fatigue strength due to the low amplitude oscillatory sliding motion between contacting surfaces. Fretting commonly occurs in clamped joints and shrink fitted components. The fretting fatigue properties of a material are generally established via the generation of S/N curves, both fretted and unfretted, for the relevant contacting materials. A number of factors are known to influence fretting fatigue strength: these include contact pressure, range of slip and particular material combinations (1). Previous investigations have attempted to quantify fretting fatigue strength in terms of these parameters (2, 3 for example) but no laws have been established which could be used to predict the fatigue life of a component under fretting conditions. Factors such as range of slip are also very difficult or impossible to measure on components under service conditions.

It has been demonstrated that small cracks (<1 mm in depth) can form at an early stage in fatigue life (4, 5). Non-propagating cracks have also been observed in specimens tested at stresses below the fretting fatigue limit (3, 6). It may be therefore that under certain circumstances, fretting fatigue performance is governed by the conditions for propagation of these defects. Despite the small size of the defects, it may be possible to develop a method of assessing the conditions for growth based on the use of fracture mechanics. Such a method has been applied by Edwards, Ryman and Cooke (5) to predict the crack propagation lives of aluminium alloy fretting fatigue assemblies. A similar approach has been adopted by the present workers (7, 8) to calculate the critical size of defect which can grow under fretting conditions. The method involves comparing the applied stress intensity factor range (ΔK_{APP}) with experimentally determined threshold stress

* Central Electricity Generating Board, Central Electricity Research Laboratories, Leatherhead, Surrey, England.

intensity (ΔK_o) at the appropriate value of stress ratio. For such a method to be successful in predicting fretting fatigue strength the crack initiation phase of life must also be considered. Here the conditions for the formation and the nature of the small fretting defects require investigation. This aspect is the subject of the present paper.

EXPERIMENTAL PROCEDURE

Fatigue specimens of the type shown in Fig. 1 were machined from a 3½NiCrMoV steel. Bridge type fretting contact pads, Fig. 2, of span(S) equal to 12.7, 25.4 or 50.8 mm were machined from 1CrMo steel, thus giving an actual fretting materials combination which can occur in some large generators (6). The composition and mechanical properties of the two steels are given in Tables 1 and 2.

Table 1: Chemical Composition of Fatigue Specimen and Contact Pad Steels

Element (wt.%)	C	Si	Mn	S	P	Ni	Cr	Mo	V
Fatigue Specimen	0.21	0.25	0.30	0.006	0.010	3.43	1.57	0.41	0.12
Contact Pad	0.42	0.30	0.59	0.022	0.030	0.29	1.42	0.75	-

Table 2: Room Temperature Mechanical Properties of 3½NiCrMoV and 1CrMo Steels

	0.2% Proof Stress (MPa)	Tensile Strength (MPa)	Elongation %	Redn. in area %	Hardness VPN
3½NiCrMoV	600	733	25	70	222
1CrMo	841	999	21	59	340

Contact Pads were clamped to the ground flats on the specimen using a calibrated steel proving ring, Fig. 3. Nominal contact pressures of 30 and 300 MPa were employed. Fretting fatigue tests were carried out in an Amsler Vibrophore test machine, at approximately 150 Hz cyclic frequency. During a fretting fatigue test, fluctuating frictional forces are generated between specimen and fretting pad feet. These were monitored by strain gauges attached to the underside of the fretting pad, Fig. 2. Each pad was calibrated using a technique in which a static load applied to a split specimen is diverted entirely through the fretting pads. During a fretting fatigue test the approximately sinusoidal strain output from each gauge was recorded using a transient recorder. Thus the range of frictional force present at each pad foot (ΔF_t) was determined continuously throughout each test. The relative slip range between pad foot and specimen was also determined using this data to allow for pad deflection and load

redistribution from specimen to pad.

EXPERIMENTAL RESULTS AND DISCUSSION

Fatigue Testing

In a previous study (6), base line fatigue S/N data were collected for the 3½NiCrMoV steel together with fretting fatigue results for the 3½NiCrMoV/1CrMo combination. Contact pressures of 30 and 300 MPa were employed at a pad span of 25.4 mm. This study has now been extended to include fretting fatigue results for pad spans of 12.7 and 50.8 mm. Test results are summarised in Table 3.

Table 3: Fatigue Test Results

Pad Span (mm)	Applied Mean Stress (MPa)	Applied Contact Pressure (MPa)	Fatigue Limit* (MPa)	
Unfretted	0	-	±300	
Unfretted	300	-	±215	
25.4	0	30	±140	Ref. 6
25.4	300	30	± 60	
25.4	0	300	±140	
25.4	300	300	± 60	
50.8	0	30	≃ ±140**	
50.8	300	30	± 50	
12.7	0	30	±160	
12.7	300	30	±120	

* Defined as stress amplitude for 10^8 cycles endurance

** Approximate value as severe fretting wear of contact pad was encountered.

In order to determine the conditions governing the initiation and early growth of small fretting defects a number of further fretting fatigue tests have been made at applied stresses below the fretting fatigue limits given in Table 3. Specimens were cycled at the chosen stress for 10^7 cycles and were then broken open to reveal any fretting defects. Defects were either broken open after cooling the specimen in liquid nitrogen or by continuing the fatigue test at a much elevated stress, after removal of the fretting assembly.

Frictional Force Measurements

A typical plot of frictional force range (ΔF_t) versus endurance in a fretting fatigue test is shown in Fig. 4. The frictional force always exhibits a mean value of zero, independent of applied mean stress. A rise in ΔF_t is sometimes observed in the early stages of the test ($<10^5$ cycles) until an approximately constant valve is achieved. This "plateau" value is maintained throughout the test provided initiation of a major fatigue crack does not occur. In the latter situation, as illustrated in Fig. 4, the

frictional force measured on the side of crack initiation can fall rapidly.

The plateau value of frictional force was determined for all conditions of alternating stress, contact pressure and pad span. Plots of this value versus applied stress amplitude are given in Fig. 5. The measurements indicate that the peak frictional force ($\Delta F_t/2$) achieves a limiting value approximately equal to the applied contact load on each pad foot. This implies that a maximum coefficient of friction equal to unity is achieved under fretting conditions at a stress amplitude greater than some critical value which itself is dependent on pad span. This finding is in agreement with those of Edwards and Cooke (9) and Endo et al., (10).

Metallography and Fractography

Fretting between pads and specimen results in four rectangular fretting scars on each specimen. A longitudinal metallographic section through a scar, Fig. 6, exhibits typical fretting fatigue cracks which initially grow almost parallel to the specimen surface before gradually rotating towards a plane perpendicular to the applied stress axis. Cracks tend to initiate at the outer edge of the pad before growing beneath the foot.

Fractographic observations were made using both optical and scanning electron microscopy of 'broken-open' fretting defects produced during the interrupted fretting fatigue tests carried out at stresses below the fretting fatigue limit. A typical fretting defect is shown in Fig. 7. In this case the specimen was broken open after cooling in liquid nitrogen and the tip of the fretting defect is marked by the change in fracture mode. Fretting defects were also broken open by continuing the fatigue test at much elevated stress, after removal of the fretting pads, Fig. 8. The fretting crack tip is then marked by an abrupt change in crack angle, the non-fretting 'break-open' fracture being perpendicular to the specimen surface.

The very shallow angle to the specimen surface initially adopted by the fretting defects is apparent in both Figs. 7 and 8. The fracture surface of the defects at depths less than about 50 μm is comparatively smooth and can exhibit a series of ridges running parallel to the direction of crack growth, Fig. 9. These features are possibly indicative of shear or stage I type of crack. At crack depths greater than 50 μm the fracture is more typical of high cycle fatigue in this material. However the crack remains under the influence of mixed mode loading due to the fretting assembly, since the fatigue crack plane changes angle abruptly as soon as the fretting pads are removed, Fig. 8. The entire surface of the fretting crack is covered with patches of oxide, which probably arises from wear between contacting surfaces rather than from fretting of the crack surfaces.

Defect Size Measurements

The depth (measured perpendicular to the specimen surface) of the largest defect broken open in any one specimen was determined by optical microscopy. In most cases this defect was the largest of several exposed by breaking open as many defects as possible in each of the four fretting scars produced in a test. The defect aspect ratio (depth divided by semi-surface length) was also measured. The results are presented in Table 4 in order of increasing defect size.

Defect aspect ratio is in all cases less than unity and can be as low as 0.06, the shallow defect then extending over almost the entire fretting scar width. This indicates a high driving force for crack growth along the surface.

Defect sizes are given in Table 4 in order of increasing depth. No correlation exists between defect depth and externally applied stresses. Defect depth is however related to the plateau value of frictional force range, ΔF_t, determined from Fig. 5. Note that the largest defects are found at 300 MPa contact pressure due to the increased level of ΔF_t and despite a reduction in slip range. Slip range therefore apparently has no significance in determining defect depth. The relationship between depth and ΔF_t is given in Fig. 10. Frictional force range must largely control the range of localised surface stresses in the region below the fretting pad foot and hence governs defect formation. Since this friction stress must decay rapidly below the surface, crack arrest occurs at externally applied stresses below the fretting fatigue limit. The present data are insufficient to determine the precise role of applied contact pressure but it may be that increased contact pressure tends to close defects angled beneath the pad foot, thus acting to reduce their eventual size in comparison with defects produced at lower contact pressure and equivalent ΔF_t.

Table 4: Maximum Defect Sizes Measured in Interrupted Fretting Fatigue Tests

Maximum Defect Depth (mm)	Defect Aspect Ratio	Applied Stress (MPa)	Applied Contact Pressure (MPa)	Pad Span (mm)	Plateau ΔF_t (N)	Range of Slip (μm)
Unable to Break-open	-	300 ± 50	30	25.4	420	5.1
"	-	0 ± 70	30	25.4	515	7.3
0.08	0.14	150 ± 90	30	25.4	621	9.5
0.10	0.7	0 ± 90	30	25.4	617	9.5
0.13	0.4	0 ± 110	30	25.4	714	11.7
0.16	0.18	0 ± 80	30	50.8	892	16.4
0.16	0.4	0 ± 90	30	50.8	893	18.8
0.18	0.25	0 ± 140	30	25.4	827	15.0
0.20	0.06	0 ± 110	300	25.4	2050	8.7
0.22	0.3	0 ± 130	300	25.4	2319	10.5

Fretting Fatigue Assessment

The significance of the defects in terms of fretting fatigue failure assessment is demonstrated in Fig. 11. Maximum expected defect sizes, governed by ΔF_t, are superimposed on a typical fretting fatigue S/N curve. This demonstrates that at stresses considerably below the fretting fatigue limit defects are initiated and can grow to a depth of around 0.1 mm before arresting. As applied stresses are increased the depth to which the defect can grow is increased until, at stresses very close to the fatigue limit, a maximum defect depth of approximately 0.18 mm is expected. As stress is increased further, complete specimen failure must result from the continued propagation of such a defect.

Fracture mechanics computations (5, 8) do not predict a reduction in crack driving force ($\Delta K_{APP} - \Delta K_o$) over this range of crack sizes and hence the arrest of these small defects cannot be predicted by linear elastic fracture mechanics (LEFM). It may be possible however to use LEFM concepts to describe the continued growth of the defects. This approach is being pursued using LEFM to calculate the critical defect size which can grow at the fretting fatigue limit and comparing this value with the fretting defect size.

Conclusions

(1) Fretting fatigue experiments indicate that small surface defects can initiate at stresses considerably below the fretting fatigue limit.

(2) The size of these defects is related to the frictional force between fretting specimen and contact pad and is independent of externally applied stresses, over the range investigated.

(3) The small defects grow initially at a shallow angle to the specimen surface by a shear mode of crack extension. The defects are highly extended along the specimen surface.

(4) The results indicate that fretting fatigue may be assessed by consideration of the conditions for continued propagation of these defects.

ACKNOWLEDGEMENTS

This work was carried out at the Central Electricity Research Laboratories and is published by permission of the Central Electricity Generating Board.

REFERENCES

1. Waterhouse, R.B., Fretting Corrosion, Pergamon 1972.
2. Nishioka, K. and Hirakawa, K., Bull. JSME 12 (1969) 692.
3. Nishioka, K. and Hirakawa, K., Proc. Int. Conf on Mech. Behaviour of Materials Kyoto Japan. Japan. Soc. Mat. Sci (1972) 308.
4. Endo, K. and Goto, H., Wear 38 (1975) 311.

5. Edwards, P.R., Ryman, P.J. and Cooke, R. RAE Tech. Rpt. 77056 (Royal Aircraft Establishment Farnborough England, 1977).
6. King, R.N. and Lindley, T.C., "Advances in Fracture Research". Proc. ICF5. Ed D. Francois, Pergamon Press, London (1980). 631.
7. Lindley, T.C. and Nix, K.J. ASTM STP. To be published 1984.
8. Nix, K.J. and Lindley, T.C. "The Application of Fracture Mechanics to Fretting Fatigue". CERL Note in press (1984).
9. Edwards, P.R. and Cooke, R., RAE Tech. Rpt. 78019. (Royal Aircraft establishment Farnborough England, 1978).
10. Endo, K., Goto, H. and Fukunaga, T. Bull. JSME 17 (1974) 108.

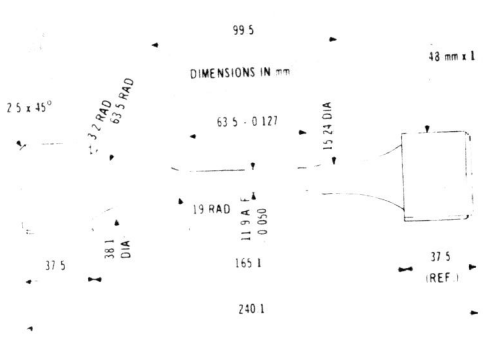

FIG. 1 FATIGUE SPECIMEN

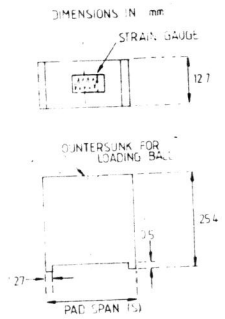

FIG.2 BRIDGE TYPE CONTACT PAD

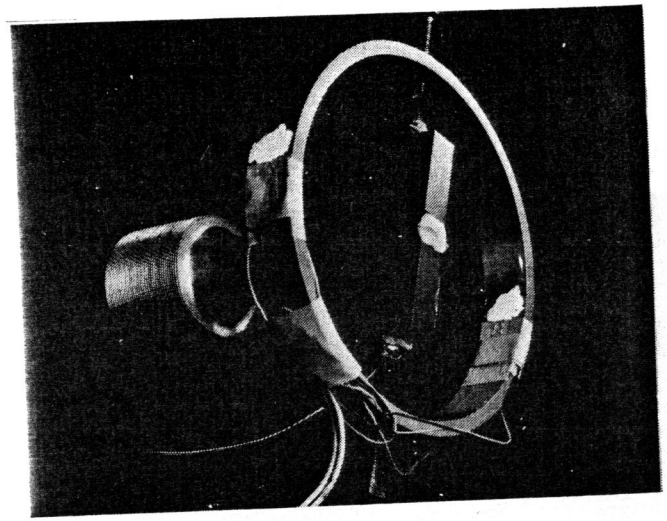

Fig. 3: Proving Ring Assembly

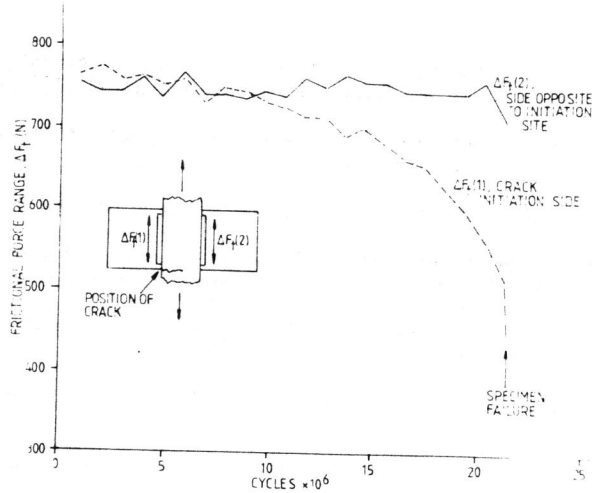

Fig. 4: Variation in Frictional Force with Endurance in a Fretting Fatigue Test. Applied stress = 300 ± 55 MPa. Pad Span = 50.8 mm

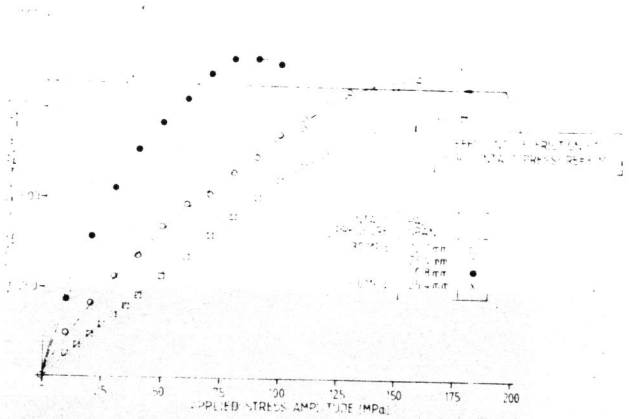

Fig. 5: Relationship Between Plateau Value of Frictional Force and Applied Stress

Fig. 6: Metallographic section through a Fretting Scar showing Fretting Cracks (Specimen Nickel Plated)

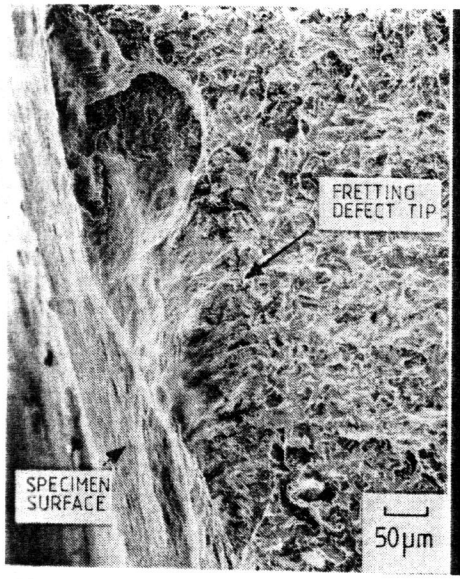

Fig. 7: Small Fretting Defect Broken Open by Brittle Fracture

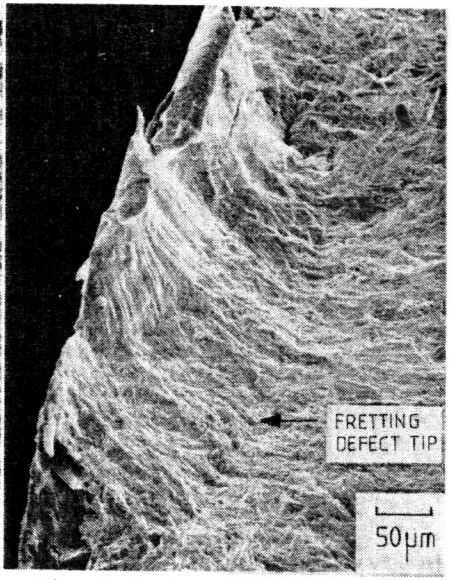

Fig. 8: Small Fretting Defect Broken Open by Fatigue at Elevated Stress

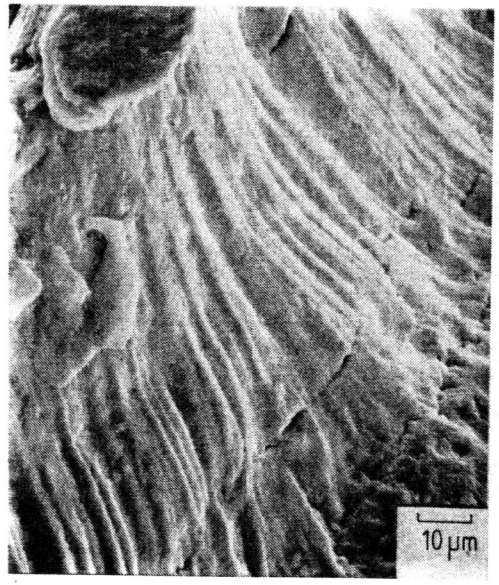

Fig. 9: Detail from Fig. 8 of Fracture Close to Origin

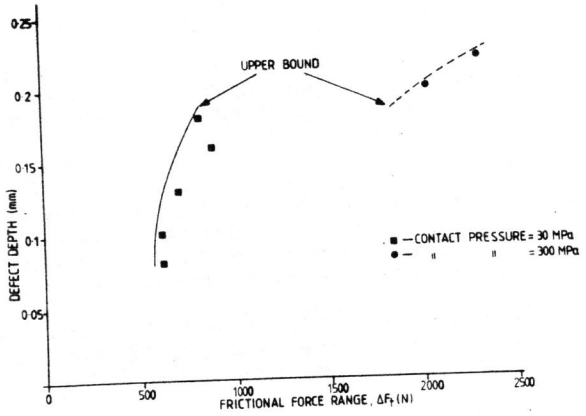

Fig. 10: Fretting Defect Size as a function of applied Frictional Force Range

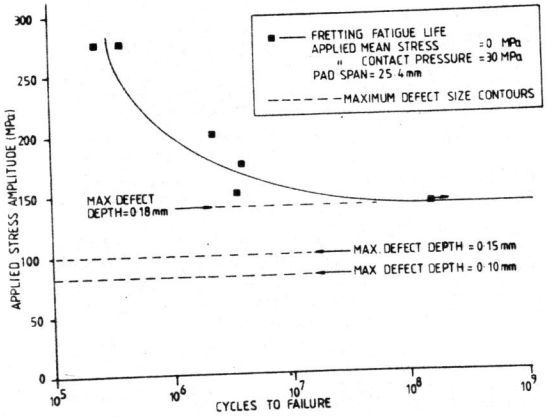

Fig. 11: Typical Fretting Fatigue S/N Curve Superimposed with Fretting Defect Size Contours